Otopro Volume 21 No. 2 May 2026 pages. 43-50
P-ISSN: 1858-411x; E-ISSN: 2685-7863
DOI: 10.26740/otopro.v21n2.p43-50 https://journal.unesa.ac.id/index.php/jo
(This journal accommodates review, experimental, and thinking related to mechanical engineering and its application)

EFFECT OF SECTION THICKNESS ON NODULAR GRAPHITE FORMATION AND MECHANICAL PROPERTIES OF DUCTILE CAST IRON

Moch. Chamim [1*], *Edi* Sarwono[1], *Haikal*[1] and *Margono*[1]

[1]Mechanical Engineering Study program, Sekolah Tinggi Teknologi "Warga" Surakarta, Central Java, Indonesia
chamim@sttw.ac.id

Abstract. This study investigates the effect of section thickness on the microstructure and mechanical response of Ductile Cast Iron (DCI) using specimens with thicknesses of specimen 20, 40, and 60 mm. Optical microscopy reveals a ferrite-pearlite matrix with spherical graphite, where the graphite nodules exhibit a tendency toward larger size and greater heterogeneity with increasing section thickness. The measured nodule diameters are approximately 17-20 µm (20 mm), 21-22 µm (40 mm), and 15-26 µm (60 mm), indicating thickness-driven changes in solidification/cooling conditions that promote graphite hardening in thicker sections. Mechanical testing shows a consistent decrease in hardness with increasing thickness: 246.8 VHN (specimen 20 mm), 226.75 VHN (specimen 40 mm), and 204.8 VHN (specimen 60 mm). Impact test results show a non-monotonic trend, increasing from 0.02 (specimen 20 mm) to 0.049 (specimen 40 mm) and slightly decreasing to 0.045 (specimen 60 mm). The highest impact value at specimen 40 mm indicates an optimal balance between matrix hardness and toughness at intermediate thicknesses, while the slight decrease at specimen 60 mm despite the lower hardness may be related to increased graphite size heterogeneity and microstructural nonuniformity in thicker sections. Overall, thickness significantly affects graphite morphology and the hardness toughness trade off in DCI, with 40 mm sections providing the most favorable toughness in this data set.

Keywords: DCI; Graphite; Microstructure; Thickness; Hardness.

1 Introduction

Ductile Cast Iron (DCI) is widely used in automotive components, machinery, and structures due to its favorable combination of strength [1], ductility [2], and castability[3]. Unlike gray cast iron/Ferro Casting (FC), which contains flake graphite that acts as a stress concentrator, ferro casting ductile contains spherical (nodular) graphite that significantly improves mechanical performance by reducing crack initiation and propagation [4], [5]. The spherical graphite morphology is achieved through proper magnesium treatment and inoculation, which promotes graphite nucleation during solidification [6]. Due to these microstructural characteristics, ferro casting ductile exhibits mechanical properties close to those of cast steel while maintaining the economic advantages of cast iron [7].

In casting processes, microstructure formation is strongly influenced by solidification conditions [8]. One of the most critical parameters governing solidification behavior is cross-section thickness. According to solidification theory and Chvorinov's rule, the cooling rate decreases with increasing cross-section thickness due to the larger volume-to-surface area ratio [9]. In gray cast iron and steel castings, variations in section thickness are known to affect graphite morphology, grain size, segregation behavior, and ultimately mechanical properties [10]. Thicker sections typically experience slower cooling rates, resulting in coarser microstructures and different phase distributions compared to thinner sections [11].

In DCI material, the influence of section thickness is more complex because it directly affects graphite nucleation density, nodule size, nodularity index, and matrix transformation (ferrite-pearlite balance) [12]. Slower cooling in thicker sections can reduce the number of nodules and increase their size, potentially altering mechanical performance. Conversely, thinner sections tend to solidify more rapidly, which can refine the graphite distribution but also modify the matrix

* Corresponding author: chamim@sttw.ac.id

phase depending on the thermal gradient [9], [13], [14]. These microstructural variations are closely related to changes in hardness, as hardness in ferro casting ductile is primarily governed by the matrix structure while indirectly influenced by graphite morphology [3].

Most previous studies have investigated the effects of chemical composition, magnesium treatment, and inoculation practices on graphite formation [5], [10], [15], [16], [17]. Only a small number of studies have systematically examined the influence of geometric section thickness under identical casting conditions, particularly in sand casting processes representative of industrial practice. In real engineering components, section thickness variations frequently occur within a single casting, leading to non-uniform cooling histories and potentially heterogeneous microstructures. However, the direct, isolated effects of thickness variations independent of compositional or processing changes remain insufficiently clarified. Furthermore, previous studies generally report monotonic relationships between thickness and mechanical parameters such as hardness or strength, while the combined response of hardness and impact toughness across different section thicknesses is rarely addressed. In particular, the possibility that intermediate thicknesses may provide an optimal balance between hardness and toughness has received little attention. Furthermore, many studies emphasize the average graphite size or nodularity index, while the role of graphite size heterogeneity associated with cross-sectional thickness and its implications for impact behavior is rarely analyzed in detail.

2 Material and methods

2.1 Material

The specimens were made of Ductile Cast Iron (DCI) produced by local industry. The specimen pattern is made in layers with different dimensions thicknesses as shown in Figure 1. The process of making specimens is simultaneously one tapping with the manufacture of sand molds so that the material is the same. The specimens made include the chemical composition (Table 1) test specimen of the spectrometer.

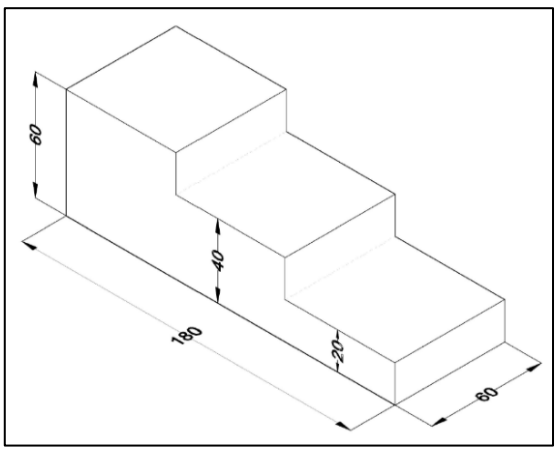

Fig. 1. Specimen pattern design dimension in mm.

Table 1. Chemical composition of specimen

Element	Weight (wt.%)	St. Dev
Fe	92.15	0.187
C	3.680	0.061
Si	3.741	0.135
Mn	0.182	0.004
Ni	0.070	0.0013
Mg	0.040	0.011
Cr	0.036	0.005
S	0.020	0.0028
Mo	0.015	0.0042

2.2 Experimental Methods

The casting pattern was designed with three section thicknesses (20, 40, and 60 mm), as shown in Figure 1, and all specimens were extracted from the corresponding regions of the as-cast block produced in one melt and one pouring operation. For metallographic analysis, samples from each thickness section were cut, ground, polished, and etched using 2 mL HNO_3 and 20 mL alcohol for 3-5 second, then observed by optical microscopy at 100x, 200x, and 500x magnification. Hardness testing was performed on the cross-section of each specimen according to ASTM E384 using a Micro-Vickers hardness tester with a load of 9.8 kgf. Four repeated measurements were taken at the central region of each cross-section, and the reported hardness value was the average of these four measurements. Charpy V-notch impact specimens (10×10×55mm) were prepared from each thickness section in accordance with ASTM E23-02a. The impact test was repeated three times for each thickness, and the reported value represents the average of the three results.

3 Results and discussion

3.1 Metallography analysis at different thickness

The metallographic observations at 100x, 200x, and 500x magnification (Figures 2-10) show that all specimens consist predominantly of spheroidal graphite embedded in a ferrite-pearlite matrix. This indicates that the melt treatment was effective in promoting nodular graphite formation under the present casting conditions. In ductile cast iron, the matrix constitution and graphite morphology are both strongly influenced by thermal history during solidification and subsequent solid-state transformation [8], [9], [13].

The observed microstructural variations among the 20, 40, and 60 mm sections are consistent with the effect of section thickness on local cooling conditions. As section thickness increases, the volume-to-surface-area ratio becomes larger, reducing the cooling rate and extending local solidification time in accordance with solidification theory and Chvorinov-type behavior [9]. Under such conditions, section thickness affects not only graphite nucleation and growth during solidification, but also matrix evolution during eutectoid transformation.

For the 20 mm specimen, the graphite nodules observed at 500× magnification were relatively small, with measured diameters of approximately 17–20 µm. This behavior was consistent with the faster cooling expected in thinner sections. A higher cooling rate generally promotes more extensive graphite nucleation while restricting the growth of individual nodules, resulting in a finer graphite distribution [9], [13]. The relatively finer graphite morphology in the 20 mm section is therefore metallurgically consistent with its smaller cross-section.

In the 40 mm specimen, the measured nodule size increases slightly to approximately 21–22 µm. This trend suggests that the lower cooling rate in the thicker section provided a longer time for graphite growth compared with the 20 mm section. The microstructure still consists of spheroidal graphite within a ferrite–pearlite matrix, but the increase in nodule size indicates that section thickness had already begun to influence graphite growth kinetics.

The 60 mm specimen shows the broadest nodule size variation, with measured diameters ranging from approximately 15 to 26 µm. This broader size distribution suggests that, in addition to overall graphite coarsening, the thickest section experienced greater local heterogeneity in thermal history. In thicker cast sections, slower and less uniform heat extraction may produce local variations in nucleation density and growth time, leading to a wider distribution of graphite nodule size [8], [9]. Thus, the present results suggest that increasing thickness does not simply enlarge graphite nodules on average, but may also increase the heterogeneity of the graphite population.

From a metallurgical perspective, the effect of cooling rate is not limited to graphite morphology. In as-cast ductile iron, cooling through the eutectoid transformation range strongly influences the ferrite-pearlite balance. Faster cooling generally tends to favor a relatively more pearlitic or finer transformed matrix, whereas slower cooling provides more time for carbon diffusion from austenite toward graphite, thereby promoting ferrite formation [8]. Although ferrite and pearlite fractions were not quantitatively measured in the present study, the observed changes in hardness discussed below are consistent with this general metallurgical interpretation.

Overall, the metallographic results indicate that section thickness affects ductile cast iron microstructure through two coupled mechanisms: (1) modification of graphite nucleation and growth during solidification and (2) alteration of matrix evolution during cooling after solidification. The thinner section tends to produce finer graphite and a relatively harder matrix, whereas the thicker sections tend to exhibit coarser and more heterogeneous graphite together with a softer matrix response.

3.2 Hardness test at different thickness

The Micro-Vickers hardness values decrease progressively with increasing section thickness, namely 246.8 VHN for the 20 mm specimen, 226.75 VHN for the 40 mm specimen, and 204.8 VHN for the 60 mm specimen (Figure 11). This trend indicates that section thickness has a significant effect on hardness in the present ductile cast iron casting.

The higher hardness of the 20 mm specimen is consistent with the faster cooling expected in the thinnest section. In ductile cast iron, hardness is governed primarily by matrix constitution, especially the relative proportions and morphology of ferrite and pearlite, while graphite morphology exerts a secondary but still important influence [3], [13], [14]. Under faster cooling, the eutectoid transformation proceeds under more limited diffusion conditions, which generally favors a relatively harder matrix response. Conversely, in thicker sections, slower cooling allows more time for carbon redistribution, which tends to promote a softer matrix and hence lower hardness [8], [13].

The present hardness results therefore support the metallographic interpretation that increasing section thickness reduced the cooling rate and shifted the microstructure toward a softer condition. However, because ferrite and pearlite fractions were not quantitatively determined, this explanation should be interpreted as being consistent with the metallurgical behavior reported in the literature rather than as a directly measured phase-fraction result. This distinction is important for maintaining consistency between the experimental evidence and the interpretation.

In addition to matrix evolution, the graphite morphology may also contribute indirectly to the hardness trend. The finer graphite distribution in the 20 mm section and the coarser, more heterogeneous graphite observed in the thicker sections can modify the local stress distribution during indentation. Nevertheless, the dominant explanation for the hardness decrease with thickness is most reasonably attributed to the effect of cooling rate on matrix transformation.

3.3 Impact test result of different thickness

The impact test results show that section thickness also affects the impact resistance of the material (Figure 12). The average impact values are 0.02 J/mm² for the 20 mm specimen, 0.049 J/mm² for the 40 mm specimen, and 0.045 J/mm² for the 60 mm specimen. Unlike the hardness values, which decrease monotonically with thickness, the impact response shows a non-monotonic trend, increasing from 20 mm to 40 mm and then decreasing slightly at 60 mm.

The low impact value of the 20 mm specimen is consistent with its highest hardness. In metallic materials, an increase in hardness is often associated with reduced ability to accommodate plastic deformation before fracture. In the present case, the thinner section likely developed a relatively harder matrix under faster cooling, which may have reduced impact energy absorption.

The 40 mm specimen exhibits the highest impact value, suggesting that this intermediate thickness provided the most favorable balance between hardness and toughness among the three conditions studied. From a microstructural standpoint, this result can be

interpreted as an intermediate condition in which the matrix became sufficiently less hard to permit greater energy absorption, while graphite heterogeneity had not yet become as pronounced as in the 60 mm specimen.

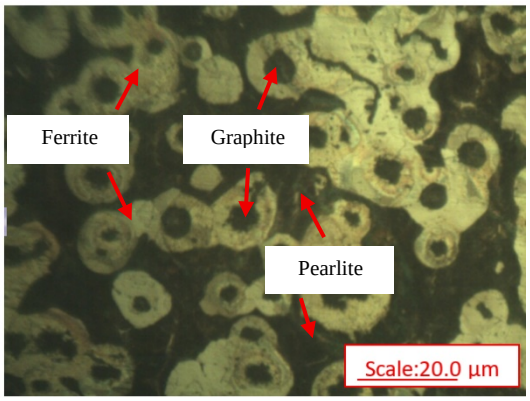

Fig. 2. Microstructure DCI 20 mm 100x magnification.

Fig. 3. Microstructure DCI 20 mm 200x magnification.

Fig. 4. Microstructure DCI 20 mm 500x magnification.

Although the 60 mm specimen has the lowest hardness, its impact value does not exceed that of the 40 mm specimen. This indicates that impact toughness in ductile cast iron is not controlled by matrix softness alone. Graphite size heterogeneity, local non-uniformity in transformed microstructure, and possible casting-related discontinuities may all influence crack initiation and propagation during impact loading [2], [11]. In the present study, the wider graphite size variation observed in the 60 mm section provides a plausible explanation

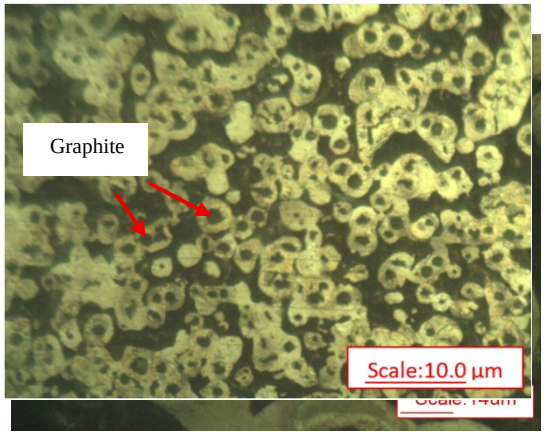

for the slight reduction in impact performance relative to the 40 mm specimen. However, since defects such as porosity or shrinkage were not specifically characterized, their role cannot be confirmed and should not be overstated.

The standard deviation values for the thicker specimens also indicate a relatively wide scatter in the impact response. Therefore, the impact trend should be interpreted as a general tendency rather than as evidence of a sharply separated mechanical regime. Additional repetition and quantitative characterization of graphite nodule count, ferrite-pearlite fraction, and casting defects would help strengthen the mechanistic interpretation of the impact behavior.

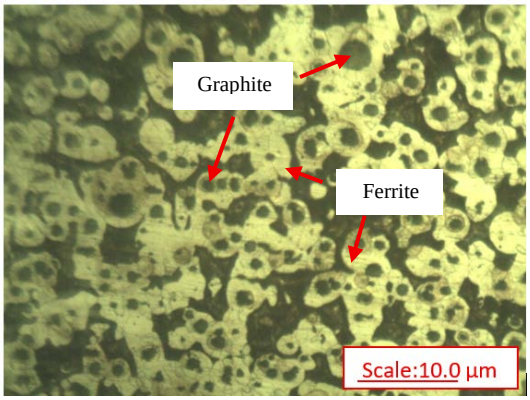

Fig. 5. Microstructure DCI 40 mm 100x magnification.

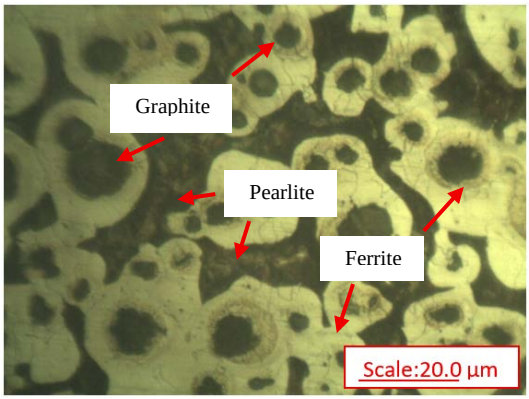

Fig. 6. Microstructure DCI 40 mm 200x magnification.

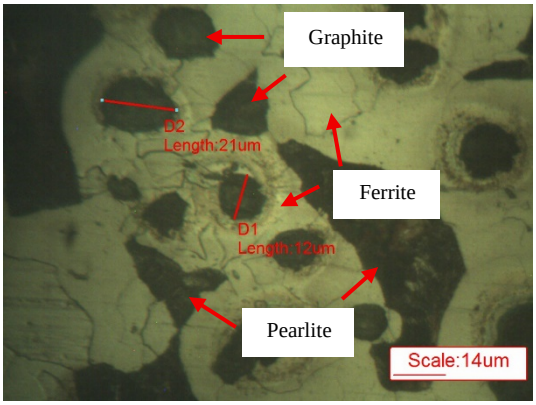

Fig. 7. Microstructure DCI 40 mm 500x magnification.

3.4 Influence of thickness on microstructure–property relationship

The relationship between microstructure and mechanical properties in the present study can be

interpreted through the combined effect of graphite evolution and matrix transformation under different cooling conditions. Section thickness affects local cooling rate, and this in turn influences both graphite nucleation/growth and ferrite-pearlite development [8], [9], [13].

The 20 mm specimen, which cooled the fastest, showed finer graphite nodules and the highest hardness. This behavior is consistent with a relatively harder transformed matrix. The 40 mm specimen showed slightly coarser graphite, lower hardness, and the highest impact value, indicating that an intermediate cooling condition may provide a more favorable compromise between deformation resistance and toughness. The 60 mm specimen exhibited the lowest hardness but also a slight decline in impact performance compared with the 40 mm specimen. This suggests that excessive slowing of the cooling rate may reduce hardness but may also increase graphite size heterogeneity and microstructural non-uniformity, which can reduce the benefit of a softer matrix during impact loading.

Therefore, the influence of thickness in the present ductile cast iron casting should not be described simply as “thicker sections are softer.” A more precise metallurgical interpretation is that increasing section thickness progressively modifies the balance between graphite size/distribution and matrix constitution. The final mechanical response results from the interaction of these features rather than from a single structural parameter alone. Within the range studied, the 40 mm section appears to provide the most balanced combination of hardness and impact resistance.

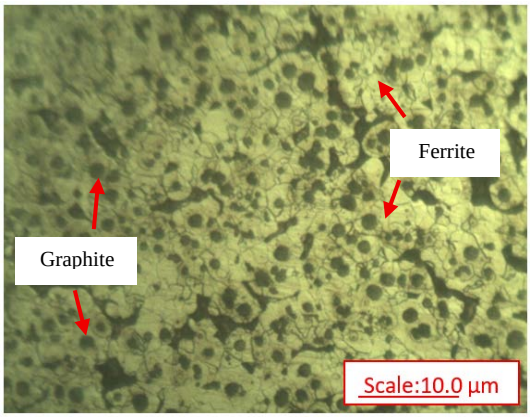

Fig. 8. Microstructure DCI 60 mm 100x magnification.

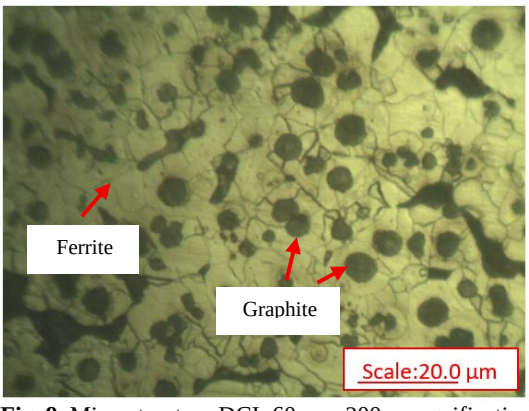

Fig. 9. Microstructure DCI 60 mm 200x magnification.

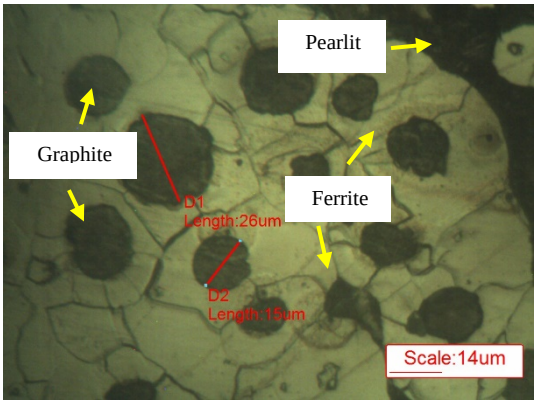

Fig. 10. Microstructure DCI 60 mm 500x magnification.

Specimen 20 mm thickness, nodule measurements at 500× magnification show relatively small diameters (marked examples: D1 ≈ 20 µm and D2 ≈ 17 µm). Mechanistically, thinner sections generally cool more rapidly, allowing for easier graphite nucleation and more “controlled” nodule growth (nodules tend to be finer). The research data also indicates that the 20 mm specimen has the highest "relative amount of graphite," which is due to rapid cooling, which helps maintain the graphite's spherical shape.

Specimen 40 mm thickness, the marked nodule sizes become slightly larger (e.g., ≈ 21–22 µm in the two measurements listed). This makes sense, as the thicker section provides a longer graphite growth time than the 20 mm specimen. Visually, the ferrite-pearlite matrix remains visible, so the most noticeable change here is a trend toward graphite enlargement compared to the thinner specimen, although more nodule measurements are needed to determine a "statistical increase."

Specimen 60 mm thickness, the graphite size data you marked shows a broader distribution: there are relatively large nodules (D1≈26 µm) but also small ones (D2≈15 µm). This pattern often occurs when cooling is slower and local conditions across a thick section become less uniform (e.g., temperature gradients and transformation times vary across regions), allowing some nodules to grow larger while others remain smaller. Thus, not only does the average increase, but size heterogeneity can also increase at greater thickness.

3.5 Hardness test at different thickness

Micro-Vickers hardness testing was conducted at a load of 9.8 kgf with four indentations made at different locations on each specimen (Figure 11). The average measured hardness values decreased with increasing section thickness, namely 246.8 VHN for the 20 mm specimen, 226.75 VHN for the 40 mm specimen, and 204.8 VHN for the 60 mm specimen. The higher hardness in the thinner section is associated with a faster cooling rate, while the lower hardness in thicker sections is attributed to slower cooling and the development of a relatively softer matrix.

The results of Micro-Vickers hardness testing on DCI materials demonstrate a strong influence of section thickness on hardness values. The hardness values obtained were 246.8 VHN for a thickness of specimen

20 mm, 226.75 VHN for specimen 40 mm, and 204.8 VHN for 60 mm. Thus, there is a decreasing trend in hardness with increasing thickness, with the thinnest specimens exhibiting the highest hardness and the thickest specimens the lowest.

Metallurgically, this trend can be explained by differences in cooling rates during solidification due to variations in thickness. At specimen 20 mm thickness, cooling is relatively faster, promoting the formation of a "harder" matrix, both through an increased tendency for pearlite formation and the possibility of the formation of hard phases such as carbides under rapid cooling conditions. Conversely, at thicker sections (specimen 40-60 mm), slower cooling allows for longer carbon diffusion times, thus austenite transformation tends to produce a relatively softer matrix.

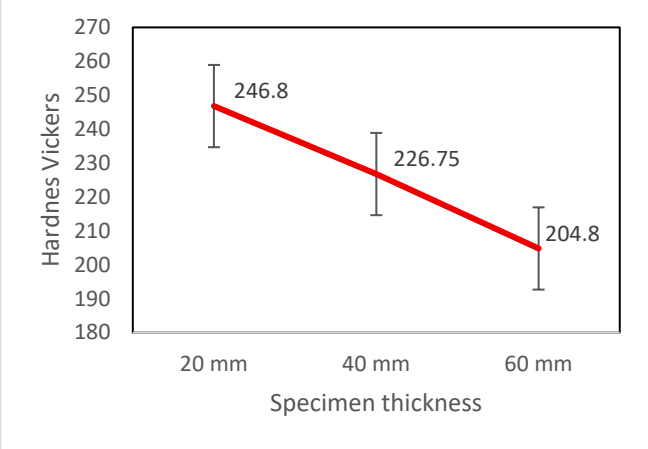

Fig. 11. Hardness value different thickness specimen.

3.6 Impact test result of different thickness

Impact test results (Figure 12) specimen indicate that cross-sectional thickness affects the material's ability to absorb impact energy. Based on data from three tests, specimen 20 mm had impact values of 0.02 J/mm2. The specimen 40 mm produced values of 0.049 J/mm2. While the 60 mm specimen produced values of 0.045. In general, impact values increased sharply from specimen 20 mm to specimen 40 mm, then decreased slightly at specimen 60 mm, but remained higher than at specimen 20 mm.

The increase in impact values from specimen 20 mm to specimen 40 mm can be discussed as an indication of increased toughness at intermediate thicknesses, consistent with microstructural changes resulting from differences in cooling rates. At thinner thicknesses, the material tends to exhibit "harder" behavior (20 mm also has the highest hardness), so the energy absorbed before fracture tends to be lower. As thickness increases to specimen 40 mm, the matrix structure generally becomes more capable of plastic deformation (more "ductile" relative to the thinnest state), so the absorbed impact energy increases and reaches its highest average value at this state.

Interestingly, at specimen 60 mm, the impact values do not reach their highest values, even though (based on experiment hardness data) this specimen is the softest. This pattern makes sense considering that impact toughness is controlled not only by matrix "softness," but also by other microstructural factors that increase crack sensitivity for example, wider variation in graphite size across thickness (in your microstructural data, specimen 60 mm indicates the presence of nodules that can be larger and more heterogeneous), and possible local nonuniformities that facilitate crack initiation. Furthermore, the standard deviation of 0.03 at specimen 40 mm and specimen 60 mm indicates a fairly wide spread of results (there are "outlier" values such as 0.086 at specimen 40 mm and 0.074 at specimen 60 mm), so the interpretation of the trend should be read as a general trend, not a completely stable difference. To strengthen claims in manuscripts, it is common to add more replications or supporting analyses (e.g., defect/pore examination and quantification of graphite nodules and pearlite-ferrite fractions) to further confirm the thickness-microstructure-impact value relationship.

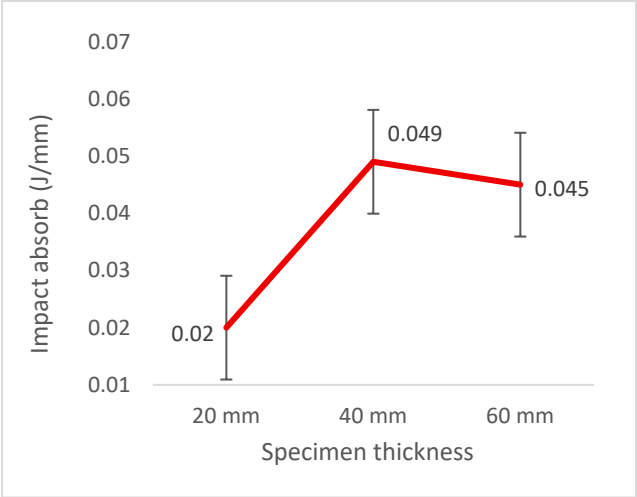

Fig. 12. Impact test of specimen in different thickness.

3.7 Influence of thickness to properties

The relationship between microstructure and mechanical properties is clearly evident in your Micro-Vickers hardness data: the hardness decreases from 246.8 VHN (specimen 20 mm) to 226.75 VHN (specimen 40 mm) and 204.8 VHN (specimen 60 mm). Metallurgically, this decrease is consistent with a tendency for the matrix to become relatively less "hard" as cooling slows (e.g., a decrease in the pearlite fraction or differences in the character of the pearlite/carbides formed). Your document also explicitly links this trend to the effect of thickness on pearlite formation and the effect of rapid cooling on the formation of harder structures.

Meanwhile, the impact test graph in your data shows a trend of increasing impact values from specimen 20 mm to specimen 40 mm, then a slight decrease at specimen 60 mm. This "peak at intermediate thickness" pattern is consistent with a common trade-off: as a material becomes harder (as at specimen 20 mm), impact toughness often decreases due to more brittle behavior; as thickness increases to specimen 40 mm and the matrix becomes more softer ductile (decreasing hardness), the absorbed impact energy can increase. The

specimen 60 mm is not the highest despite having the lowest hardness. From a microstructural perspective, one plausible explanation is the presence of large, heterogeneous nodules (e.g., 26 µm vs. 15 µm) that can amplify local stress concentrations, and thick sections are often at risk of micro-casting defects (e.g., porosity) that are highly sensitive to impact yield strength but this latter point should be read as a possibility, as it requires evidence of micro-defects (e.g., observation of pores/shrinkage) for confirmation.

Metallurgically, this trend can be explained by differences in cooling rates during solidification due to variations in thickness. At specimen 20 mm thickness, cooling is relatively faster, promoting the formation of a "harder" matrix, both through an increased tendency for pearlite formation and the possibility of the formation of hard phases such as carbides under rapid cooling conditions. Conversely, at thicker sections (specimen 40-60 mm), slower cooling allows for longer carbon diffusion times, thus austenite transformation tends to produce a relatively softer matrix.

4 Conclusion

Based on microstructural observations and mechanical property testing of DCI materials with varying thicknesses of specimen 20mm, specimen 40mm, and specimen 60 mm, it can be concluded that cross-sectional thickness significantly affects the characteristics of nodular graphite, the ferrite-pearlite matrix, as well as the hardness and impact resistance responses. Increasing thickness indicates a tendency for graphite nodule size to increase and heterogeneity to increase, as evidenced by the graphite size variations at specimen 20 mm (≈17–20 µm), specimen 40 mm (≈21–22 µm), and specimen 60 mm (≈15–26 µm). These changes demonstrate the effect of different cooling rates, with thicker cross-sections cooling more slowly, allowing for longer graphite growth times and resulting in greater nodule size variation.

In line with the microstructural changes, the micro-Vickers hardness values consistently decreased with increasing thickness, reaching 246.8 VHN (specimen 20 mm), 226.75 VHN (specimen 40 mm), and 204.8 VHN (specimen 60 mm). This trend indicates that thin sections tend to form a harder matrix, while thicker sections form a relatively softer/more ductile matrix, generally related to the shift in ferrite-pearlite composition due to differences in cooling rates during solidification.

Impact test results indicate that toughness does not increase monotonically with thickness. The average impact value increases from 0.02 (specimen 20 mm) to 0.049 (specimen 40 mm), then decreases slightly at 0.045 (specimen 60 mm). The peak toughness at specimen 40 mm thickness indicates more optimal microstructural conditions for absorbing impact energy, while the slight decrease at specimen 60 mm thickness, despite being softer, may be attributed to increased graphite size heterogeneity and possible microstructural non-uniformities in the thick sections, which could facilitate crack initiation. Overall, specimen 40 mm thickness provided the most balanced combination of mechanical properties in this study, namely moderate hardness with the highest impact value, thus potentially being a more optimal cross-sectional condition for applications requiring a compromise between deformation resistance and toughness.

References

[1] T. Mojisola, S. O. Seidu, P. A. Olubambi, and A. A. Adediran, “Effect of preconditioning on the microstructure and mechanical properties of ductile cast iron,” *Mater. Today Proc.*, vol. 62, pp. S23–S29, Jan. 2022, doi: 10.1016/j.matpr.2022.02.081.

[2] M. Y. Abdellah *et al.*, “Mechanical Properties and Fracture Toughness Prediction of Ductile Cast Iron under Thermomechanical Treatment,” *Metals (Basel).*, vol. 14, no. 3, Mar. 2024, doi: 10.3390/met14030352.

[3] X. Wang *et al.*, “Relationship among process parameters, microstructure, and mechanical properties of austempered ductile iron (ADI),” *Materials Science and Engineering: A*, vol. 857, Nov. 2022, doi: 10.1016/j.msea.2022.144063.

[4] P. K. Jena *et al.*, “Microstructure, mechanical and ballistic property evaluation of a high strength low alloy steel produced through continuous casting route,” *Advances in Materials and Processing Technologies*, vol. 8, no. 1, pp. 427–443, 2022, doi: 10.1080/2374068X.2020.1815135.

[5] M. I. Boulifa and A. Hadji, “Study of the influence of alloying elements on the mechanical characteristics and wear behavior of a ductile cast iron,” *Frattura ed Integrita Strutturale*, vol. 15, no. 56, pp. 74–83, 2021, doi: 10.3221/IGF-ESIS.56.06.

[6] S. P. S. Singh Sivam, A. Rajasekaran, S. RajendraKumar, K. SathiyaMoorthy, and M. Gopal, “A study of cooling time, copper reduction and effects of alloying elements on the microstructure and mechanical properties of SG iron casting during machining,” *Australian Journal of Mechanical Engineering*, vol. 19, no. 1, pp. 10–18, 2021, doi: 10.1080/14484846.2018.1560679.

[7] ASM International, “Asm metals handbook, vol 09 metallography and microstructure,” *Metals Handbook*, 1985.

[8] T. Borsato, P. Ferro, A. Fabrizi, F. Berto, and C. Carollo, “Long solidification time effect on solution strengthened ferritic ductile iron fatigue properties,” *Int. J. Fatigue*, vol. 145, Apr. 2021, doi: 10.1016/j.ijfatigue.2020.106137.

[9] E. Colin-García, R. G. Sánchez-Alvarado, A. Cruz-Ramírez, M. A. Suarez-Rosales, L. Portuguez-Pardo, and J. C. Jiménez-Lugos, “EFFECT OF REGULAR THICKNESSES ON THE MICROSTRUCTURAL AND QUANTITATIVE ANALYSIS FOR A HYPO-EUTECTIC DUCTILE IRON ALLOYED WITH

Ni AND V," *Journal of Mining and Metallurgy, Section B: Metallurgy*, vol. 60, no. 1, pp. 15–31, 2024, doi: 10.2298/JMMB231114002C.
[10] I. Lichioiu, "Evaluation of Graphite Distribution-Part Thickness Ratio in Gray Cast Irons Microstructure," *RECENT - REzultatele CErcetărilor Noastre Tehnice*, vol. 24, no. 3, pp. 256–259, 2023, doi: 10.31926/RECENT.2023.71.256.
[11] Y. B. Zhang *et al.*, "Microstructure and residual elastic strain at graphite nodules in ductile cast iron analyzed by synchrotron X-ray microdiffraction," *Acta Mater.*, vol. 167, pp. 221–230, Apr. 2019, doi: 10.1016/j.actamat.2019.01.038.
[12] J. Zhang *et al.*, "The influence of cooling rate on microstructure and magnetic properties of cast Fe-6.5wt%Si steel," in *Journal of Physics: Conference Series*, Institute of Physics, 2023. doi: 10.1088/1742-6596/2635/1/012026.
[13] J. Bai *et al.*, "Microstructures and Mechanical Properties of Ductile Cast Iron with Different Crystallizer Inner Diameters," *Crystals (Basel).*, vol. 12, no. 3, Mar. 2022, doi: 10.3390/cryst12030413.
[14] B. Wang, G. C. Barber, F. Qiu, Q. Zou, and H. Yang, "A review: Phase transformation and wear mechanisms of single-step and dual-step austempered ductile irons," *Journal of Materials Research and Technology*, vol. 9, no. 1, pp. 1054–1069, Jan. 2020, doi: 10.1016/j.jmrt.2019.10.074.
[15] O. J. Akinribide, S. O. O. Olusunle, S. O. Akinwamide, B. J. Babalola, and P. A. Olubambi, "Impact of heat treatment on mechanical and tribological behaviour of unalloyed and alloyed ductile iron," *Journal of Materials Research and Technology*, vol. 14, pp. 1809–1819, Sep. 2021, doi: 10.1016/j.jmrt.2021.07.077.
[16] K. Dong, C. Lu, W. Zhou, D. O. Northwood, and C. Liu, "Wear behavior of a multiphase ductile iron produced by quenching and partitioning process," *Eng. Fail. Anal.*, vol. 123, May 2021, doi: 10.1016/j.engfailanal.2021.105290.
[17] L. Horbach *et al.*, "The effect of silicon on the critical resolved shear stress of solid solution strengthened ferritic ductile iron," *Mater. Des.*, vol. 244, Aug. 2024, doi: 10.1016/j.matdes.2024.113130.